# *PIK3CA* C2 domain deletions hyperactivate phosphoinositide 3-kinase (PI3K), generate oncogene dependence and are exquisitely sensitive to PI3Kα inhibitors

**Sarah Croessmann**[1], **Jonathan H. Sheehan**[2,3], **Kyung-min Lee**[1], **Gregory Sliwoski**[4], **Jie He**[5], **Rebecca Nagy**[7], **David Riddle**[1], **Ingrid Mayer**[1,8], **Justin M. Balko**[1,8], **Richard Lanman**[7], **Vincent A. Miller**[5], **Lewis C. Cantley**[9], **Jens Meiler**[3,4], and **Carlos L. Arteaga**[1,6,8,*]

[1]Department of Medicine, Vanderbilt University, Nashville, TN

[2]Department of Biochemistry, Vanderbilt University, Nashville, TN

[3]Center for Structural Biology, Vanderbilt University, Nashville, TN

[4]Department of Biomedical Informatics, Vanderbilt University, Nashville, TN

[5]Foundation Medicine, Inc, Cambridge, MA

[6]Department of Cancer Biology, Vanderbilt University, Nashville, TN

[7]Guardant Health, Inc, Redwood, CA

[8]Breast Cancer Program, Vanderbilt-Ingram Cancer Center, Vanderbilt University, Nashville, TN

[9]Meyer Cancer Center of Weill Cornell Medical College, New York, NY

## Abstract

**Purpose**—We describe herein a novel P447_L455 deletion in the C2 domain of *PIK3CA* in a patient with an ER+ breast cancer with an excellent response to the PI3Kα inhibitor alpelisib. Although *PIK3CA* deletions are relatively rare, a significant portion of deletions cluster within amino acids 446–460 of the C2 domain, suggesting these residues are critical for p110α function.

**Design**—A computational structural model of PIK3CA[delP447-L455] in complex with the p85 regulatory subunit and MCF10A cells expressing PIK3CA[delP447-L455] and *PIK3CA*[H450_P458del] were used to understand the phenotype of C2 domain deletions.

---

[*]Corresponding Author: Carlos L. Arteaga, MD, Division of Oncology, Vanderbilt University Medical Center, 2220 Pierce Avenue, 777 PRB, Tel: 615-343-6653, Fax: 615-343-7602.

**Results**—Computational modeling revealed specific favorable inter-residue contacts that would be lost as a result of the deletion, predicting a significant decrease in binding energy. Co-immunoprecipitation experiments showed reduced binding of the C2 deletion mutants with p85 compared to wild type p110α. The MCF10A cells expressing PIK3CA C2 deletions exhibited growth factor-independent growth, an invasive phenotype, and higher phosphorylation of AKT, ERK and S6 compared to parental MCF10A cells. All these changes were ablated by alpelisib treatment.

**Conclusions**—C2 domain deletions in *PIK3CA* generate PI3K dependence and should be considered biomarkers of sensitivity to PI3K inhibitors.

## Introduction

*PIK3CA* is the most mutated gene in breast cancer with an overall rate of ~40%. More than 80% of these mutations are located in 'hot spots' within exons 9 and 20 in the helical and kinase domain, respectively (1,2). The remainder of *PIK3CA* mutations are widely distributed over its entire coding sequence (3). *PIK3CA* encodes the p110α catalytic subunit, which dimerizes with the p85α regulatory subunit and induces the formation of the second messenger phosphatidylinositol (3,4,5)-trisphosphate (PIP3)(4). Hot spot mutations in *PIK3CA* have been shown to partially destabilize the association of p110α with p85 and, thus, relieve the enzymatic activity of p110α from p85-mediated inhibition (5–7). This results in increased residence time of p110α at the plasma membrane, enhanced formation of PIP3, and subsequent hyper activation of AKT/mTOR signaling, resulting in growth-factor independent growth, cellular transformation, invasion and metastases (8–10).

Early studies showed that mutations in the C2 domain make up less than 5% of *PIK3CA* mutations and also enhance kinase activity (3). However, more recent next generation sequencing studies suggest that C2 domain mutations make up greater than 10% of *PIK3CA* mutations (Table S1). Rudd *et al* first reported PIK3CA[delP447_L455] in ovarian cancer and observed that it was associated with higher levels of phosphorylated AKT than the more common C2 domain missense point mutation E453K (11). Although deletions occur in only 3% of *PIK3CA* mutations, a significant portion of these deletions occur in a small range of critical residues within the C2 domain. This is equivalent to approximately 1100 new breast cancers per year. Herein, we report that deletions in the C2 domain of *PIK3CA* result in disruption of p85α binding, increased p110α activity and cellular transformation As a result, cells harboring these alterations are highly vulnerable to treatment with PI3K inhibitors. These data have important implications for the selection of patients for trials with therapies targeted to the PI3K/AKT pathway.

## Methods

### Cell lines

MCF10A breast epithelial cells (ATCC® CRL-10317[TM]; purchased in 2012) were from ATCC. Cell lines were authenticated by ATCC prior to purchase by the short tandem repeat (STR) method. Isogenically modified MCF10A cells containing *PIK3CA* E545K or H1047R were developed previously (12). The Gateway cloning system (Thermo Fisher Scientific)

was used to generate pLX302-*PIK3CA* plasmids encoding *PIK3CA*$^{\text{WT}}$ and the two C2 deletions, *PIK3CA*$^{\text{P447\_L455del}}$ and *PIK3CA*$^{\text{H450\_P458del}}$. Transfected MCF10A cells were maintained in MCF10A complete media (DMEM/F12 supplemented with 5% horse serum, 20 ng/ml EGF, 10 μg/ml insulin, 0.5 μg/ml hydrocortisone, 0.1 μg/ml cholera toxin, and 1x Pen/Strep). For experiments, 2% charcoal/dextran-stripped serum (CSS) serum was used, and EGF and insulin were removed as indicated. Experiments were carried out on cells with passage numbers below 20.

## Cell line generation

The pDONR-223 vector encoding *PIK3CA*$^{\text{WT}}$ was subjected to site-directed mutagenesis (Genewiz) to generate *PIK3CA*$^{\text{P447\_L455del}}$ and *PIK3CA*$^{\text{H450\_P458del}}$. The *PIK3CA*$^{\text{WT}}$ and mutant plasmids were recombined into the lentiviral expression vector pLX-302 containing a C-terminal V5 epitope tag. Lentiviral supernatant was produced in early-passage 293FT cells by transfection with psPAX2 and pMD2.G packaging plasmids along with the generated pLX302-*PIK3CA* plasmids. Viral supernatant was filtered and applied to MCF10A cells in the presence of polybrene. After 48 h, cells were selected with 1.5 μg/mL puromycin and tested for plasmid expression via immunoblot analysis with a V5 antibody. Stable cell lines were maintained in media containing 1 μg/mL puromycin.

## Determination of *PIK3CA* C2 deletions and mutations

The frequency of *PIK3CA* C2 deletions and mutations was determined using cBioPortal (13) (including METABRIC and Genie), COSMIC (14), and databases from Foundation Medicine and Guardant Health.

## Computational modeling

Structural modeling of the *PIK3CA*$^{\text{P447\_L455del}}$ was performed using Rosetta. The experimental crystal structure complex of p110α and p85α (PDBID: 3HIZ) was used to examine the binding interface of wild type proteins and deletion mutants. The N-terminal expression tag was removed prior to modeling and all mutated residues were reverted to wild-type. Finally, the structure was refined with Rosetta's FastRelax protocol while constraining backbone atoms to their crystallographic coordinates. To model deletion mutants, residues corresponding to 447–455 (447del) and 450–458 (450del) were removed; resulting chain breaks were fused with cyclic coordinate descent (CCD) followed by kinematic refinement in Rosetta. All conditions were refined once more with constraints to starting coordinates with 3000 trajectories and a final ensemble of 1000 models was selected based on overall pose energy. To quantitate changes in interface energy between the three conditions, the dG_separated (change in energy between isolated and chains in complex) was calculated with the Interface Analyzer application; the top ten models per condition by dG_separated were compared. To identify specific interactions lost in the deletions, Residue Energy Breakdown was run for all models. Residue pairs contributing to at least 0.1 Rosetta Energy Units (REU) across the interface in the wild type, and not in a deletion mutant, were considered as potentially lost interactions.

## Immunoblot analysis

Cells were washed with PBS and lysed on ice in NP-40 lysis buffer plus protease and phosphatase inhibitors. Protein concentrations were measured using BCA protein assay reagent (Pierce). Lysates were subjected to SDS-PAGE and transferred to nitrocellulose membranes (Invitrogen) as previously described (15). Immunoreactive bands were detected by enhanced chemiluminescence following incubation with horseradish peroxidase-conjugated secondary antibodies. Primary antibodies included: V5 Tag (CS13202), p110α (CS4249), p85 (CS4257), p-p70S6K (CS9205), p90RSK (CS9333), PathScan® Multiplex Western Cocktail I (for p-AKT S473, p-p90RSK, p-ERK, and p-S6), GAPDH. The Invitrogen NuPage system was used. Nitrocellulose membranes were cut horizontally to probe with multiple antibodies.

## Cell growth assay

For dose response curves to generate an $IC_{50}$, cells were seeded in 96-well plates at a density of 200 cells per well in growth factor depleted media. The next day, media was replaced with media containing 1 μM alpelisib ± EGF and/or Insulin as indicated. Media and growth factors were changed every 3 days. Cells were stained using crystal violet, resuspended in 1% SDS, and imaged using a GloMax plate reader. Additional growth assays were carried out in 12-well dishes at a seeding density of 2000 cells/well. Growth assays were quantified using a LiCOR Odyssey Infrared plate reader. For three-dimensional (3D) growth assays, cells were seeded on growth factor-reduced matrigel (BD Biosciences) in 8-well chamber slides as described previously [11].

## Statistical analysis

All experiments were performed using three technical replicates and at least two independent times. P values were calculated using GraphPad Prism (version 6.0) by ANOVA followed by Tukey's multiple comparisons test.

## Co-Immunoprecipitation

Cell lysates were harvested using ice cold lysis buffer (1% Triton X-100, 10% Glycerol, 100 mM NaCL, 50 mM HEPES, 100 mM Na3VO4, 10 mM NaF, 1 Roche Minitab) and rotated at 4°C for 1 h. Lysates were then clarified by spinning at 10,000 xg at 4°C for 15 min. Protein concentrations were measured using BCA standard curves (Pierce). One μg anti V5-Tag antibody (Cell signaling 13202) was added to 1 mg of clarified cell lysate and rotated at 4°C overnight. 50 μL of Protein G agarose beads (Life technologies 10003D) were added to the lysates and rotated at 4°C for 4 h. Tubes were placed on magnets, washed three times with lysis buffer, and eluted in 20 μL of LDS sample buffer. Lysates were subjected to immunoblot analysis with a p85 antibody (Cell signaling 4257). Unbound lysate was analyzed via western blot for loading controls. Immunoblots were analyzed using ImageJ software.

## Thermal Shift Assay

Approximately $10^7$ cells were resuspended in 500 μL of PBS with Roche Complete protease inhibitor tab and subjected to 3 freeze/thaw cycles. Whole cell lysates were aliquoted into

PCR strips and exposed to a thermal gradient ranging from 44.5°C to 67°C. Tubes were spun down at 20,000 g for 20 min, and supernatants were collected followed by separation by SDS-PAGE.

## Results

### PIK3CA C2 domain mutations disrupt binding of p110α with p85α

A 63 year old postmenopausal woman with advanced estrogen receptor (ER) + breast cancer resistant to endocrine therapy exhibited an excellent and sustained clinical response (11 months) to the PI3Kα inhibitor alpelisib (BYL719) in combination with the aromatase inhibitor letrozole(16). Targeted capture next generation sequence (NGS) of DNA from a liver metastasis identified a P447_L455 deletion in the C2 domain of *PIK3CA* with an allele frequency of 11% (Figure 1A). *PIK3CA* C2 domain mutations have been previously underreported and deletions are frequently not reported by tumor and plasma cell-free DNA NGS panels. Interrogation of cBioPortal, Metabric, Genie, Foundation Medicine, and Guardant Health suggested that C2 domain mutations make up approximately 11% of all *PIK3CA* mutations, which is much higher than previously thought (Supp Table 1–4) (3). Unlike *PIK3CA* missense mutations, which are spread across the entire gene, *PIK3CA* deletions cluster in two specific regions, the p85α binding domain and the C2 domain (Figure 1B). Both of these regions are responsible for the contacts of p110α with its regulatory subunit, p85α.

To understand how this deletion would affect the binding to p85α, we performed computational structural modeling of the dimeric complex with *PIK3CA*$^{P447\_L455}$ using Rosetta, a computerized algorithm to model protein mutations and their interactions (17). We calculated the predicted change in free energy. The model was constructed from the X-ray crystal structure of the p110α/p85α complex (18). The deletion removes nine residues of p110α that form a loop in direct contact with p85α, resulting in the loss of six specific strong interactions between these two molecules (Figure 1C). Computational structural analysis determined four residues within the C2 domain deletion (Pro449, His450, Glu453, and Leu455) that significantly affected the interaction with p85α (Table 1). These predicted interactions include hydrogen bonds and salt bridges that we hypothesize disrupt the binding of p110α to the iSH2 domain of p85α, thus altering the regulatory effect of p85α on p110α.

To determine if the C2 domain deletion, *PIK3CA*$^{P447\_L455del}$, affects the activity of p110α through its interaction with p85α, we stably transduced MCF10A breast epithelial cells with lentiviral vectors encoding *PIK3CA* wild-type (WT), *PIK3CA*$^{P447\_L455del}$ (447del) and an additional deletion found in cbioportal, *PIK3CA*$^{H450\_P458del}$ (450del) (Figure 2A). Through sequencing, PCR and immunoblot analysis we were able to confirm the 27 base pair cDNA and 9 amino acid shift, respectively, due to each deletion (Figure 2B). In order to quantify the structural consequences of the P447_L455 deletion on binding to p85α, the average computed binding energy for the best 10 out of 3000 computational models was calculated for the deletion mutant, and compared to wild-type p110α. The deletion of the four previously mentioned residues led to the loss of seven interactions as indicated by an average change of greater than 0.1 Rosetta Energy Units (REU) (Figure 2C). Three of these interactions (His450-Asp464, His450-Tyr467, and Glu453-Lys567) had an average change

greater than 1.0 REU with strong interaction energy terms indicating the loss of electrostatic forces and hydrogen bonds (His450-Asp464 and Glu453-Lys567). Both $PIK3CA^{P447\_L455del}$ and $PIK3CA^{H450\_P458del}$ showed a statistically significant decrease in binding energy to p85α (Figure 2D). When compared to PIK3CA$^{WT}$, $PIK3CA^{P447\_L455del}$ showed a modest decrease in protein stability, while $PIK3CA^{P450\_458del}$ exhibited a statistically significant decrease (Figure 2E).

Thus, we stably transduced MCF10A cells with V5-tagged PIK3CA$^{WT}$, $PIK3CA^{P447\_L455del}$ and $PIK3CA^{P450\_458del}$. We confirmed equal expression of the V5-tagged constructs by immunoblot analysis (Supp. Figure 1). Cells transfected with $PIK3CA^{H450\_P458del}$, or '450del', exhibited slightly lower levels of the mutant protein when compared to $PIK3CA^{P447\_L455del}$. We speculate this may be due to the decrease in protein stability suggested by the previously discussed computational calculations. To support the predicted decrease in contacts between each $PIK3CA^{P447\_L455del}$ and $PIK3CA^{H450\_P458del}$ with p85α, we co-precipitated p85α with V5 antibodies from lysates of stably transduced MCF10A cells. Both MCF10A cells expressing the C2 domain deletions showed a reduction in p85α binding when compared to PIK3CA$^{WT}$ (Figure 2F). Quantification of this reduction is show in Figure 2G. In order to confirm the reduction in p85α binding, a thermal shift assay was performed in which cell lysates were subjected to a gradient of temperatures ranging from 44.5°C to 67°C. As the temperature increases, the p110α-p85 complex becomes less stable, denatures, and degrades. Both C2 deletions degraded at a lower temperature, suggesting that the p110α-p85 complex is less stable in intact cells compared to WT PIK3CA (Supp. Fig. S4).

## PIK3CA C2 domain deletions are activating and are inhibited by a PI3Kα inhibitor

MCF10A cells require EGF and insulin in order to propagate. Previous studies demonstrated that stable transduction with an activating *PIK3CA* mutation results in EGF- and/or insulin-independent growth. The ability of MCF10A cells to proliferate in the absence of growth factors has been used as an experimental surrogate of cellular transformation (12). In monolayer growth (2D) assays, MCF10A cells transfected with the *PIK3CA* C2 domain mutations exhibited a growth advantage when compared to parental MCF10A cells and to a lesser extent with MCF10A/*PIK3CA*$^{WT}$ cells (Figure 3B–E). *PIK3CA* is an oncogene; therefore, overexpression of the N-terminal tagged wild type protein is also expected to induce EGF-independent growth. However, upon removal of both EGF and insulin, only cells expressing the C2 domain mutations were able to grow (Figure 3D, 3E). Cells with each of the C2 deletions exhibited similar growth phenotypes when compared to isogenic cells expressing *PIK3CA* E545K, and *PIK3CA*, H1047R. In the absence of both EGF and insulin, cells expressing H1047R exhibited decreased growth when compared to cells with either a *PIK3CA* C2 deletion or E545K. Previous studies have shown that E545K weakens the p85-p110α interaction, thus removing inhibition of p110α and allowing it to remain active in the absence of both ligands (19). In contrast, cells with *PIK3CA* H1047R remain dependent on insulin for its activation. Similar to cells expressing either E545K and H1047R hotspot mutations (9) MCF10A cells expressing $PIK3CA^{P447\_L455del}$ or $PIK3CA^{H450\_P458del}$ showed invasive branching and irregular morphology, consistent with a transformed phenotype. Upon the removal of EGF, only cells harboring the C2 deletions

were capable of forming acini (Figure 3F). We next examined activation of the PI3K/AKT/TOR pathway in cells expressing the *PIK3CA* C2 deletions (20,21). Cells expressing *PIK3CA*[P447_L455del] or *PIK3CA*[H450_P458del] showed elevated levels of phosphorylated AKT at both the S473 and T308 sites in the absence of EGF and/or insulin (Figure 3G). Additionally, they showed elevated levels of p70S6K and p90RSK and slightly elevated levels of pERK. Collectively, these results suggest that *PIK3CA* C2 domain deletions hyperactivate the PI3K/AKT/TOR pathway and induce cell transformation.

The excellent clinical response to treatment with a PI3Kα inhibitor that was observed in the patient with breast cancer harboring *PIK3CA*[P447_L455del] (Fig. 1A) suggested such tumor was at least in part dependent on the oncogenic role of the C2 domain deletion mutant. Thus, we next examined the effect of alpelisib over a dose range on MCF10A cells expressing *PIK3CA*[P447_L455del] and *PIK3CA*[H450_P458del]. MCF10A cell viability over a dose range of alpelisib showed that cells with the *PIK3CA* C2 deletions were more susceptible to the PI3K inhibitor when compared to MCF10A/*PIK3CA*[WT] control cells in the absence of EGF ± insulin (Fig. 4A,B). These studies were conducted in the two conditions in which the C2 deletions showed the largest growth advantage (absence of EGF and absence of both EGF and insulin). Parental MCF10A cells were not included since they did not grow in the absence of EGF. Both C2 domain deletions exhibited complete growth inhibition in the presence of 1 μM alpelisib (Fig. 4C, Supp Fig. S5). Similarly, growth of cells expressing PIK3CA hotspot mutations was markedly inhibited upon treatment with 1 μM alpelisib. In 3D matrigel containing EGF and insulin, treatment with 1 μM alpelisib reduced the invasiveness of acini expressing the *PIK3CA* C2 deletions (Fig. 4D, first row). In the absence of EGF and/or insulin, the addition of alpelisib completely ablated acinar formation induced by the *PIK3CA* C2 deletions (Fig. 4D, fourth row). A decrease in p110α activity in the C2 deletions in the presence of alpelisib was confirmed by immunoblot analyses. Almost a complete loss of AKT phosphorylation in the presence of both EGF and insulin was observed for all four cell lines (Fig. 4E).

## Discussion

Following an excellent clinical response to a PI3Kα inhibitor in a patient with breast cancer harboring a *PIK3CA* delP447_L455 deletion, we report herein the function of this mutant and its implications for other alterations in the C2 domain of *PIK3CA*. Although previous studies suggested C2 domain mutations comprise less than 5% of *PIK3CA* mutations (3), the databases we report here suggest that these mutations make up over 10% of all *PIK3CA* mutations. The region around the deletion observed in the patient's cancer involves residues that are within a significant portion of deletions reported in *PIK3CA* (Supp. Fig 2). Scanning various databases we noticed that deletions in *PIK3CA* cluster in two regions, the p85 binding domain and C2 domain, both involved in binding to the p85α regulatory subunit (Fig. 1B). This non-random distribution suggests there is a selective advantage to the deletion of these two regions in *PIK3CA*. Our interrogation of the p110α-p85α interface revealed that the residues deleted in the patient's tumor strongly interacted with residues in the iSH2 domain of p85α, specifically clustering around p85α residues Y452-E462 and N564-M582 (Supp Fig. 3). When analyzing these sites of interaction, the corresponding residues binding to the amino acids within the p110α C2 domain deletion are the most

frequently mutated or deleted sites (amino acids Y452-E469 and N564-M582) in p85α, and are mutually exclusive with the C2 domain deletions (Supp. Fig. 3)(22).

Based on these data we hypothesized that deletions in the *PIK3CA* C2 domain are gain-of-function by reducing contacts with p85 and, thus, relieving p85-mediated inhibition. Other studies have suggested that mutations in the *PIK3CA* C2 domain changed the binding affinity of p110α with the lipid membrane (23,24). However, more recent structural studies of the commonly mutated C2 residue, Asn345, suggest mutations in this region would alter the interaction of p110α with p85α (6). Through computational analysis, this study also noted that Glu453, a residue with prominent interactions within the deleted region, was located at the interface between *PIK3CA* C2 and p85 iSH2; however the density for the side chains was not defined enough at the time to identify direct interactions. Furthermore, residues 581–593 of p85α (those found at the C2 deletion interface) have been proposed to constrain the location of the iSH2 domain of p85α and deletion of these residues removes these orientation constraints (25). This further suggested that mutations and, more specifically, deletions in the C2 domain directly disrupt the ability of p85α to regulate p110α. Indeed, computational structural modeling revealed that the deletion of select residues within the PIK3CA C2 domain, specifically 449–455, caused a significant decrease in the ability of p85α to bind p110α (Fig 2D, Table 1). Consistent with a reduction in p110α-p85 binding, V5 pulldowns showed an observable decrease in the co-precipitated p85α in the *PIK3CA* C2 deletion mutants (Fig. 2F,G). Additionally, both C2 deletions exhibited a decrease in their thermal stability of the p110α-p85 complex in intact cells (Supp. Fig. 4). These results support a reduction in the contacts between p110α and p85α but not a complete dissociation of the dimer as it is well established that p110α is unlikely to survive as a monomer *in vivo* (26).

Our studies also suggest that deletions in the PIK3CA C2 domain are activating, generate dependence on PI3K, and are exquisitely sensitive to PI3Kα inhibitors currently in clinical development. A reduction in p85α-mediated repression results in upregulation of the catalytic activity of p110α with subsequent enhanced activation of AKT/TOR signaling and ligand-independent growth. It was previously shown that p85α can be a critical modulator of insulin sensitivity and that changes in the stoichiometric balance of p85α and p110α can directly affect PI3K-dependent signaling and response to growth factor stimuli (27,28). It is tempting to speculate that the PIK3CA C2 deletions may be causal to the observed insulin-independent growth of transfected MCF10A cells (Figure 3D, 3E). Furthermore, the C2 deletions exhibit a comparable phenotype to the *PIK3CA* helical hotspot mutation, E545K, which has been shown to weaken the p85-p110α and, as a result, is less dependent on insulin-induced activation (19). In contrast, H1047R, does not weaken the p85-p110α interface and, therefore, remains dependent on insulin for its activation (Figure 3D, 3E).

Currently, several targeted capture next gen sequencing panels do not systematically examine deletions in *PIK3CA* in tumor DNA extracted from tissue biopsies and/or plasma. Data shown here suggest that C2 domain mutations and deletions are more prominent than previously determined (Supp Table 1, 2) (3). One implication of these findings is that PIK3CA C2 deletions may make up a portion of patients with cancers previously categorized as PIK3CA wild type. Therefore, we propose that, in addition to hot spot

PIK3CA mutations, both deletions and mutations in the C2 domain of PIK3CA should be included in comprehensive tumor gene panels so that patients with PI3K-dependent cancers and, thus, potential sensitivity to PI3K inhibitors can be identified.

## Supplementary Material

Refer to Web version on PubMed Central for supplementary material.

## Acknowledgments

## References

1. Thorpe LM, Yuzugullu H, Zhao JJ. PI3K in cancer: divergent roles of isoforms, modes of activation and therapeutic targeting. Nat Rev Cancer. 2015; 15(1):7–24. DOI: 10.1038/nrc3860 [PubMed: 25533673]

2. Samuels Y, Wang Z, Bardelli A, Silliman N, Ptak J, Szabo S, et al. High frequency of mutations of the PIK3CA gene in human cancers. Science. 2004; 304(5670):554.doi: 10.1126/science.1096502 [PubMed: 15016963]

3. Gymnopoulos M, Elsliger MA, Vogt PK. Rare cancer-specific mutations in PIK3CA show gain of function. Proc Natl Acad Sci U S A. 2007; 104(13):5569–74. DOI: 10.1073/pnas.0701005104 [PubMed: 17376864]

4. Engelman JA. Targeting PI3K signalling in cancer: opportunities, challenges and limitations. Nat Rev Cancer. 2009; 9(8):550–62. DOI: 10.1038/nrc2664 [PubMed: 19629070]

5. Huang TH, Huo L, Wang YN, Xia W, Wei Y, Chang SS, et al. Epidermal growth factor receptor potentiates MCM7-mediated DNA replication through tyrosine phosphorylation of Lyn kinase in human cancers. Cancer Cell. 2013; 23(6):796–810. DOI: 10.1016/j.ccr.2013.04.027 [PubMed: 23764002]

6. Huang CH, Mandelker D, Schmidt-Kittler O, Samuels Y, Velculescu VE, Kinzler KW, et al. The structure of a human p110alpha/p85alpha complex elucidates the effects of oncogenic PI3Kalpha mutations. Science. 2007; 318(5857):1744–8. DOI: 10.1126/science.1150799 [PubMed: 18079394]

7. Burke JE, Perisic O, Masson GR, Vadas O, Williams RL. Oncogenic mutations mimic and enhance dynamic events in the natural activation of phosphoinositide 3-kinase p110alpha (PIK3CA). Proc Natl Acad Sci U S A. 2012; 109(38):15259–64. DOI: 10.1073/pnas.1205508109 [PubMed: 22949682]

8. Miron A, Varadi M, Carrasco D, Li H, Luongo L, Kim HJ, et al. PIK3CA mutations in in situ and invasive breast carcinomas. Cancer Res. 2010; 70(14):5674–8. DOI: 10.1158/0008-5472.CAN-08-2660 [PubMed: 20551053]

9. Isakoff SJ, Engelman JA, Irie HY, Luo J, Brachmann SM, Pearline RV, et al. Breast cancer-associated PIK3CA mutations are oncogenic in mammary epithelial cells. Cancer Res. 2005; 65(23):10992–1000. DOI: 10.1158/0008-5472.CAN-05-2612 [PubMed: 16322248]

10. Liu P, Cheng H, Santiago S, Raeder M, Zhang F, Isabella A, et al. Oncogenic PIK3CA-driven mammary tumors frequently recur via PI3K pathway-dependent and PI3K pathway-independent mechanisms. Nat Med. 2011; 17(9):1116–20. DOI: 10.1038/nm.2402 [PubMed: 21822287]

11. Rudd ML, Price JC, Fogoros S, Godwin AK, Sgroi DC, Merino MJ, et al. A unique spectrum of somatic PIK3CA (p110alpha) mutations within primary endometrial carcinomas. Clin Cancer Res. 2011; 17(6):1331–40. DOI: 10.1158/1078-0432.CCR-10-0540 [PubMed: 21266528]

12. Gustin JP, Karakas B, Weiss MB, Abukhdeir AM, Lauring J, Garay JP, et al. Knockin of mutant PIK3CA activates multiple oncogenic pathways. Proc Natl Acad Sci U S A. 2009; 106(8):2835–40. DOI: 10.1073/pnas.0813351106 [PubMed: 19196980]

13. Cerami E, Gao J, Dogrusoz U, Gross BE, Sumer SO, Aksoy BA, et al. The cBio cancer genomics portal: an open platform for exploring multidimensional cancer genomics data. Cancer Discov. 2012; 2(5):401–4. DOI: 10.1158/2159-8290.CD-12-0095 [PubMed: 22588877]

14. Forbes SA, Bhamra G, Bamford S, Dawson E, Kok C, Clements J, et al. The Catalogue of Somatic Mutations in Cancer (COSMIC). Curr Protoc Hum Genet. 2008; Chapter 10(Unit 10):1.doi: 10.1002/0471142905.hg1011s57

15. Hanker AB, Estrada MV, Bianchini G, Moore PD, Zhao J, Cheng F, et al. Extracellular matrix/integrin signaling promotes resistance to combined inhibition of HER2 and PI3K in HER2+ breast cancer. Cancer Res. 2017; doi: 10.1158/0008-5472.CAN-16-2808

16. Mayer IA, Abramson VG, Formisano L, Balko JM, Estrada MV, Sanders ME, et al. A Phase Ib Study of Alpelisib (BYL719), a PI3Kalpha-Specific Inhibitor, with Letrozole in ER+/HER2-Metastatic Breast Cancer. Clin Cancer Res. 2017; 23(1):26–34. DOI: 10.1158/1078-0432.CCR-16-0134 [PubMed: 27126994]

17. Bender BJ, Cisneros A 3rd, Duran AM, Finn JA, Fu D, Lokits AD, et al. Protocols for Molecular Modeling with Rosetta3 and RosettaScripts. Biochemistry. 2016; 55(34):4748–63. DOI: 10.1021/acs.biochem.6b00444 [PubMed: 27490953]

18. Mandelker D, Gabelli SB, Schmidt-Kittler O, Zhu J, Cheong I, Huang CH, et al. A frequent kinase domain mutation that changes the interaction between PI3Kalpha and the membrane. Proc Natl Acad Sci U S A. 2009; 106(40):16996–7001. DOI: 10.1073/pnas.0908444106 [PubMed: 19805105]

19. Zhao L, Vogt PK. Hot-spot mutations in p110alpha of phosphatidylinositol 3-kinase (pI3K): differential interactions with the regulatory subunit p85 and with RAS. Cell Cycle. 2010; 9(3):596–600. DOI: 10.4161/cc.9.3.10599 [PubMed: 20009532]

20. Ikenoue T, Kanai F, Hikiba Y, Obata T, Tanaka Y, Imamura J, et al. Functional analysis of PIK3CA gene mutations in human colorectal cancer. Cancer Res. 2005; 65(11):4562–7. DOI: 10.1158/0008-5472.CAN-04-4114 [PubMed: 15930273]

21. Kang S, Bader AG, Vogt PK. Phosphatidylinositol 3-kinase mutations identified in human cancer are oncogenic. Proc Natl Acad Sci U S A. 2005; 102(3):802–7. DOI: 10.1073/pnas.0408864102 [PubMed: 15647370]

22. Mukohara T. PI3K mutations in breast cancer: prognostic and therapeutic implications. Breast Cancer (Dove Med Press). 2015; 7:111–23. DOI: 10.2147/BCTT.S60696 [PubMed: 26028978]

23. Vogt PK, Kang S, Elsliger MA, Gymnopoulos M. Cancer-specific mutations in phosphatidylinositol 3-kinase. Trends Biochem Sci. 2007; 32(7):342–9. DOI: 10.1016/j.tibs.2007.05.005 [PubMed: 17561399]

24. Gabelli SB, Huang CH, Mandelker D, Schmidt-Kittler O, Vogelstein B, Amzel LM. Structural effects of oncogenic PI3Kalpha mutations. Curr Top Microbiol Immunol. 2010; 347:43–53. DOI: 10.1007/82_2010_53 [PubMed: 20593314]

25. Shekar SC, Wu H, Fu Z, Yip SC, Nagajyothi, Cahill SM, et al. Mechanism of constitutive phosphoinositide 3-kinase activation by oncogenic mutants of the p85 regulatory subunit. J Biol Chem. 2005; 280(30):27850–5. DOI: 10.1074/jbc.M506005200 [PubMed: 15932879]

26. Yu J, Zhang Y, McIlroy J, Rordorf-Nikolic T, Orr GA, Backer JM. Regulation of the p85/p110 phosphatidylinositol 3′-kinase: stabilization and inhibition of the p110alpha catalytic subunit by the p85 regulatory subunit. Mol Cell Biol. 1998; 18(3):1379–87. [PubMed: 9488453]

27. Taniguchi CM, Tran TT, Kondo T, Luo J, Ueki K, Cantley LC, et al. Phosphoinositide 3-kinase regulatory subunit p85alpha suppresses insulin action via positive regulation of PTEN. Proc Natl Acad Sci U S A. 2006; 103(32):12093–7. DOI: 10.1073/pnas.0604628103 [PubMed: 16880400]

28. Ueki K, Fruman DA, Brachmann SM, Tseng YH, Cantley LC, Kahn CR. Molecular balance between the regulatory and catalytic subunits of phosphoinositide 3-kinase regulates cell signaling and survival. Mol Cell Biol. 2002; 22(3):965–77. [PubMed: 11784871]

## Translational Relevance

Alterations in the C2 domain represent 11% of all *PIK3CA* mutations. C2 domain deletions make up 1% of *PIK3CA* mutated breast cancers which equates to about 1100 newly diagnosed patients each year. We show herein that *PIK3CA* C2 domain deletions are oncogenic, hyperactivate PI3K, and are exquisitely sensitive to PI3K inhibitors, thus representing a biomarker of sensitivity to this class of targeted drugs.
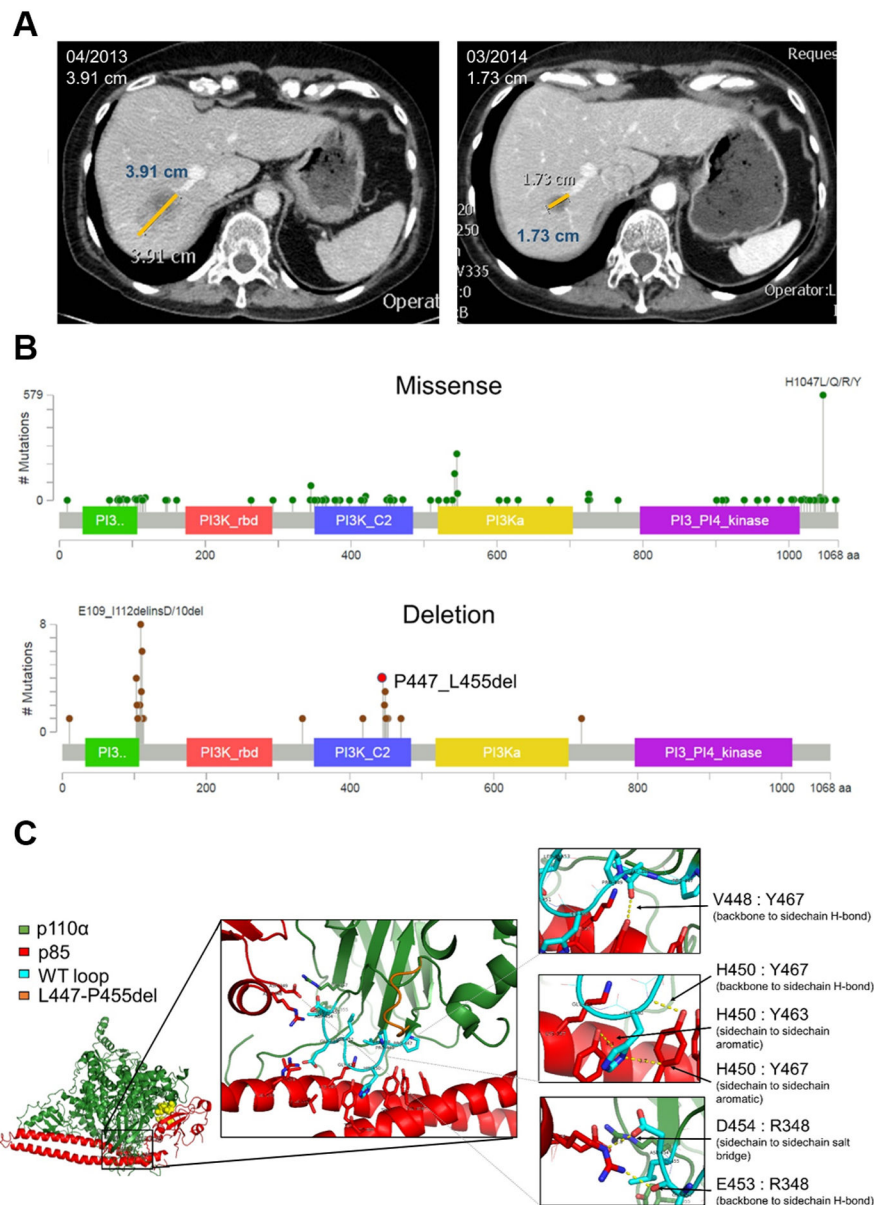
**Fig. 1. *PIK3CA* C2 deletions occur in breast cancer and cluster predominately at p85α binding sites**

(A) Liver metastasis of patient with endocrine resistant ER+ breast cancer harboring the *PIK3CA*[P447_L455del] at baseline and 11 months after starting treatment with letrozole and alpelisib. (B) Lollipop plots of *PIK3CA* missense mutations (top) and deletions (bottom) from the cBioportal database (accessed 1/2017). (C) The heterodimeric structure of p110α (green) and p85α (red). Structural analysis determined the conformation of the *PIK3CA*[WT] p110α (cyan) and the interaction with p85α is altered by the deletion, *PIK3CA*[P447-L455del] (orange). Six major interaction points (arrows) are disrupted by the loss of the nine amino acids (right).
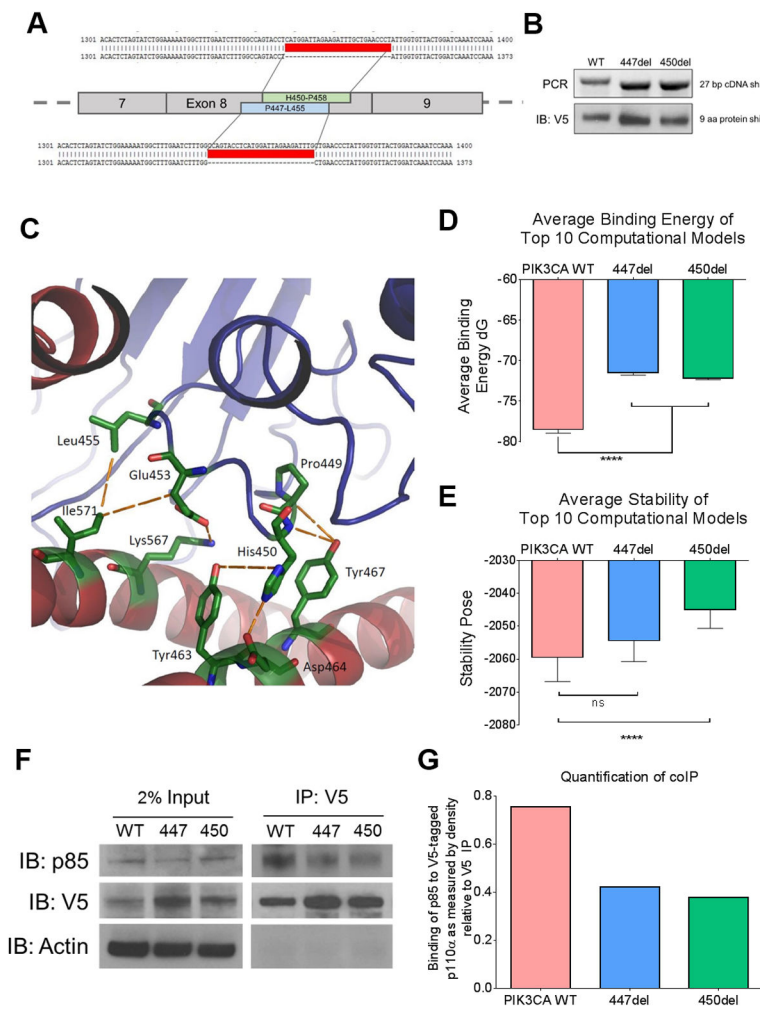
**Fig. 2. *PIK3CA* C2 deletions lead to disruption of p85α binding**

(A) Schematic representation of targeting sites of deletions in *PIK3CA*, the patient deletion, *PIK3CA*[P447_L455del] (447del) and an additional deletion from cBioportal, *PIK3CA*[H450_P458del] (450del). The Gateway cloning system was used to design constructs with V5-tag and deleted sequences were confirmed (red). MCF10A cells were infected with lentivirus to stable express the *PIK3CA*[WT] and the two deletions which will be referred to the *PIK3CA* deletion panel. (B) PCR (top) and immunoblot of V5-tag expression (bottom) confirmation of the 27 base pair DNA and 9 amino acid protein shift, respectively. (C) p110α and p85α interacting residues within *PIK3CA*[P447-L455del] . Seven main disrupted interactions are listed in Table 1. (D) Average binding energy between p110α and p85α of the top 10 computational models. Both *PIK3CA*[P447_L455del] and *PIK3CA*[H450_P458del] exhibited a statistically significant decrease in binding energy ($p<0.0001$). (E) Average calculated stability of p110α in the top 10 computational models. Only *PIK3CA*[H450_P458del] exhibited a statistically significant decrease in stability ($p<0.0001$). (F) Co-immunoprecipitation of cell lysates from MCF10A cells stably expressing *PIK3CA*[WT] or the two C2 domain deletions. Protein (1 mg) was isolated and immunoprecipitated (IP) with 1 μg anti V5-Tag antibody. Lysates were then separated with SDS-PAGE and subjected to

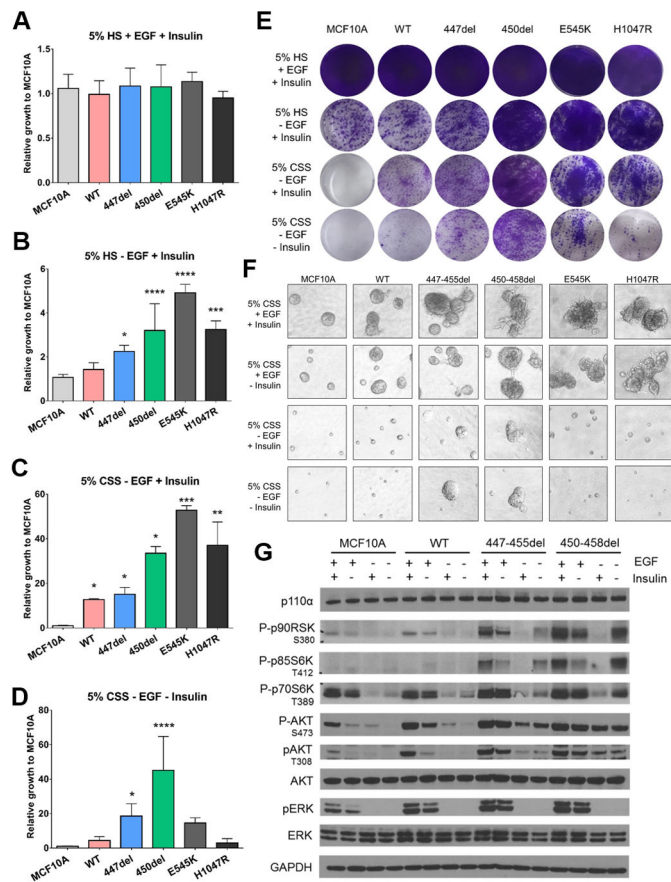immunoblot analysis (IB) with a p85α antibody. (G) Immunoblots were quantified using ImageJ.

**Fig. 3. *PIK3CA* C2 deletions are activating in breast cancer**

(A–D) Quantification of monolayer growth assay of stably transduced MCF10A cells in various media conditions lacking essential growth factors (*p > .05, ** p > .01, *** p > . 001, **** p > .0001). Cells were seeded in triplicate in 12-well plates and (E) stained on day 8 with crystal violet. (F) Parental and stably transduced MCF10A cells were plated in 3D Matrigel in MCF10A media containing 5% charcoal stripped serum (CSS) ± EGF ± Insulin. Media and growth factors were changed every 3 days. Colonies ( 50 μM) were imaged on Day 12. Assay was carried out in duplicate wells in 3 separate experiments. (G) Cells were grown in MCF10A media containing 5% CSS and ± EGF ± Insulin for 24 h. Cell lysates were subjected to immunoblot analyses with the indicated antibodies.
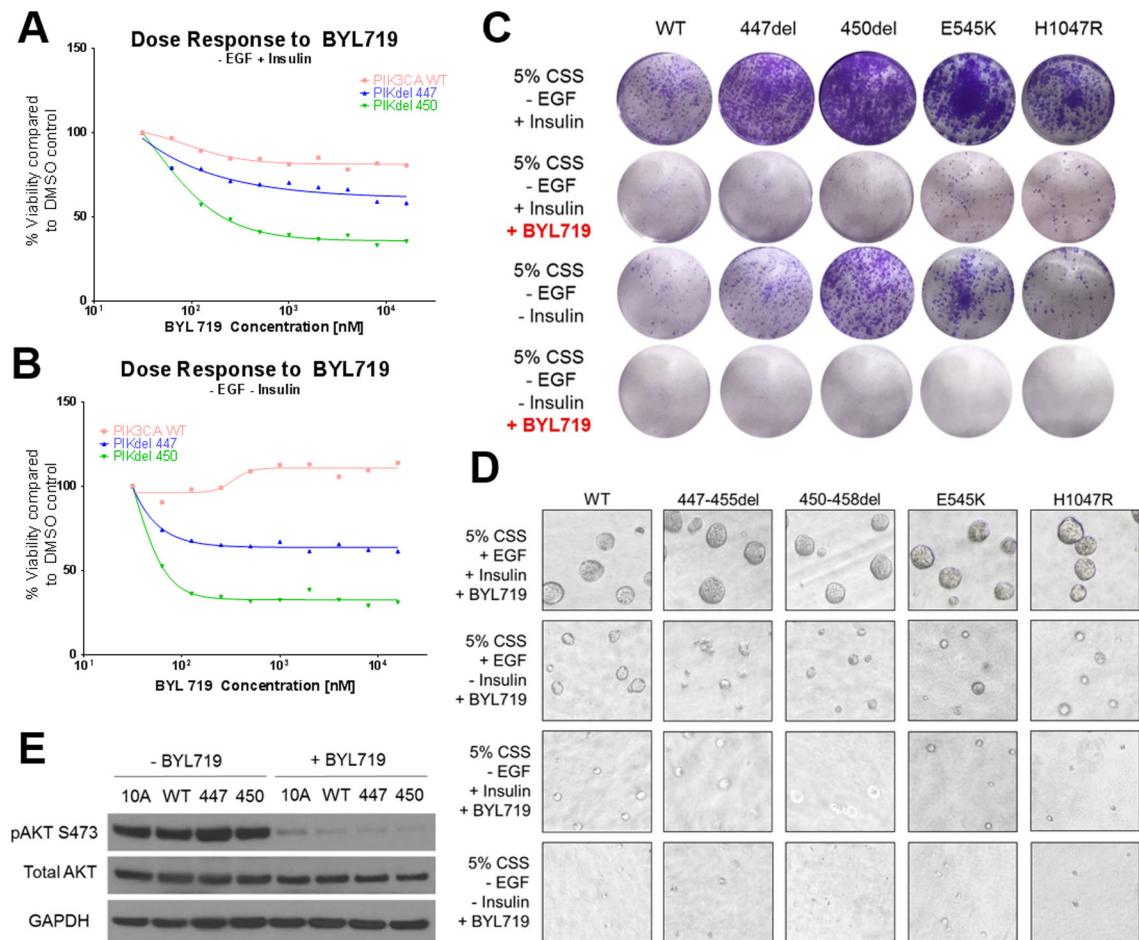
**Fig. 4. *PIK3CA* C2 deletions are sensitive to PI3Kα inhibitor alpelisib**
(A) Alpelisib dose response curve in the absence of EGF. The indicated MCF10A transfectants were seeded onto 96-well plates in triplicate and treated with increasing concentrations of alpelisib for 7 days. Plates were stained with crystal violet and resuspended in 1% sodium dodecyl sulfate (SDS) and read on a Promega GloMax Microplate reader. (B) Alpelisib dose response curve in the absence of EGF and insulin. (C) Growth assay with the *PIK3CA* deletion panel in the absence of EGF ± insulin ± 1μM alpelisib. Cells were seeded in triplicate in 12-well plates and stained on day 8 with crystal violet. Experiment was repeated 3 times. (D) Cells were plated in 3D Matrigel in MCF10A media containing 5% charcoal stripped serum (CSS) ± EGF ± insulin in the presence of 1 μM alpelisib. (E) Cells were grown in MCF10A media containing 5% CSS ± EGF ± insulin for 24 h in the presence of 1 μM alpelisib. Cell lysates were subjected to immunoblot analyses with the indicated antibodies.

**Table 1**

**Predicted destabilization of specific residue interactions at the p110α-p85α interface of both C2 deletions**

p110α and p85α interacting residues disrupted within $PIK3CA^{\text{P447-L455del}}$ (447del) and $PIK3CA^{\text{H450-P458del}}$ (450del).

| Loop Residue | p85 binding site | Average change | |
|---|---|---|---|
| | | 447del | 450del |
| Pro449 | Tyr467 | 0.41 | 0.03 |
| His450 | Tyr463 | 0.292 | 0.292 |
| | Asp464 | 1.465 | 1.465 |
| | Tyr467 | 1.815 | 1.815 |
| Glu 453 | Lys567 | 1.966 | 1.966 |
| | Ile571 | 0.114 | 0.114 |
| Leu455 | Ile571 | 0.101 | 0.101 |